Science of the Total Environment 847 (2022) 157623

Contents lists available at ScienceDirect

Science of the Total Environment

journal homepage: www.elsevier.com/locate/scitotenv

Unveiling the spatial and sectoral characteristics of a high-resolution emission inventory of CO_2 and air pollutants in China

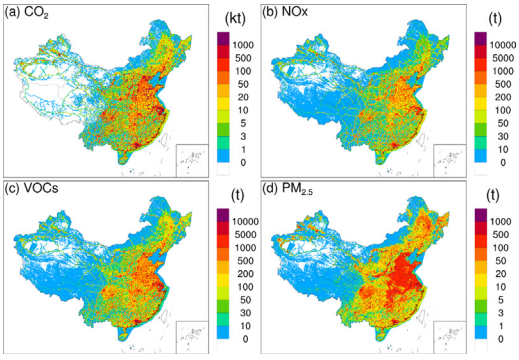
Yang Gao [a,1], Lei Zhang [a,1], Aishi Huang [a], Wenbin Kou [a], Xin Bo [b,c,*], Bofeng Cai [d,**], Jiabao Qu [e]

[a] Frontiers Science Center for Deep Ocean Multispheres and Earth System, Key Laboratory of Marine Environment and Ecology, Ministry of Education, Ocean University of China, Qingdao National Laboratory for Marine Science and Technology, Qingdao 266100, China
[b] Department of Environmental Science and Engineering, Beijing University of Chemical Technology, Beijing 100029, China
[c] BUCT Institute for Carbon-Neutrality of Chinese Industries, Beijing 100029, China
[d] Center for Carbon Neutrality, Chinese Academy of Environmental Planning, Beijing 100012, China
[e] Appraisal Center for Environment and Engineering, Ministry of Ecology and Environment, Beijing 100012, China

HIGHLIGHTS

- A high-resolution emission inventory including CO_2 and air pollutants is developed.
- 5 % of the grids in China account for 90 % of the total CO_2 emissions.
- CO_2 emissions and air pollutant emissions exhibit great spatial consistency.

GRAPHICAL ABSTRACT



ARTICLE INFO

Editor: Zhaozhong Feng

Keywords:
High-resolution emission inventory
CO_2 emissions
Air pollutants emissions
Spatial consistency
Carbon neutrality

ABSTRACT

Under the target of carbon neutrality as well as stringent air quality guideline, understanding the spatial characteristics of both greenhouse gases and air pollutants emissions, in particular of their mutual sources, is crucial for assessing the feasibility of achieving their concomitant emission control, which, nevertheless, remains to be unclear yet. To this end, we construct a high-resolution (10 km × 10 km) emission inventory including both CO_2 and air pollutants in China, which fosters us an opportunity to examine their spatial and sectoral characteristics. The primary sources for both CO_2 and air pollutant emissions are power and industry. Among different subsectors in industry, detailed information indicates cement, iron and steel are the major subsectors for both CO_2 and majority of air pollutants. Analysis of the high-resolution spatial distribution indicates that for CO_2, 5 % of the grids account for 90 % of the total CO_2 emissions, indicative of the existence of spatial heterogeneity. These grids are the major locations with air pollutant emissions as well, i.e., 73 % for SO_2 emissions, and more than 50 % for volatile organic compounds (VOCs), CO, NOx, PM_{10} and $PM_{2.5}$, stressing the spatial consistency between greenhouse gases and air pollutant emissions. A large portion of emissions concentrate in a relatively small number of grids

* Correspondence to: X. Bo, Department of Environmental Science and Engineering, Beijing University of Chemical Technology, Beijing 100029, China.
** Corresponding author.
E-mail addresses: boxin@buct.edu.cn (X. Bo), caibf@caep.org.cn (B. Cai).
[1] Authors contributed equally.

http://dx.doi.org/10.1016/j.scitotenv.2022.157623
Received 5 June 2022; Received in revised form 18 July 2022; Accepted 21 July 2022
Available online 25 July 2022
0048-9697/© 2022 Elsevier B.V. All rights reserved.

further implies the possibility to achieve the mutual control of both greenhouse gas emissions and air pollutant emissions, which is useful for future policy in particular of achieving the carbon neutrality and air quality improvement.

1. Introduction

Anthropogenic activities emit a huge amount of air pollutants and greenhouse gases especially of carbon dioxide (CO_2) into the atmosphere, exerting significant effects on climate change, socio-economy and human health (Jacob and Winner, 2009; GBD 2019 Risk Factors Collaborators, 2020). The air pollutant emissions such as carbon monoxide (CO), nitrogen oxides (NO_x), volatile organic compounds (VOCs), black carbon (BC), organic carbon (OC) and particulate matter (PM) are precursors to ozone (Sillman, 1999; Xing et al., 2011; Ma et al., 2019) and particulate matter less than or equal to 2.5 μm in diameter ($PM_{2.5}$) (Brock et al., 2002; Jimenez et al., 2009; Zheng et al., 2018; An et al., 2021). O_3 and $PM_{2.5}$ exposure are estimated to be associated with nearly 3.5 million deaths globally (Stanaway et al., 2018) and could lead to serious economic losses (Xie et al., 2019). Meanwhile, the massive emissions of CO_2 have led to global warming and further caused melting of glacial permafrost, sea level rise and extinction of some species (Root et al., 2003; Tylianakis et al., 2008; Lau et al., 2012).

China, one of the major countries with a fairly large amount of air pollutants and CO_2 emissions, has taken a series of initiatives to reduce emissions for mitigating their negative effect (Chen et al., 2017; Zheng et al., 2018). For instance, Chinese government launched the Low Carbon Cities Pilot (LCCPs) program as early as 2010, and more than 80 cities have been selected to implement a number of low-carbon policies (Chen et al., 2017; Wu et al., 2021). The implementation of several policies, like the "Eleventh Five Year Plan for National Environment Protection" and the "Action Plan on the Prevention and Control of Air Pollution", has also strengthened air quality control in China (CSC, 2007, 2013). As a result, the emission reduction of air pollutants has brought a substantial improvement in air quality (Liu et al., 2016; Li et al., 2017; Wang et al., 2017; Zeng et al., 2019; Gao et al., 2020). In contrast, the carbon emissions in China are still on the rise, making China become the country with the largest amount of carbon emissions (BP, 2020).

Facing the mutual challenges of air pollution and climate change, the Chinese government has made a commitment to the world to achieve carbon peak by 2030 and carbon neutrality by 2060, and the co-control of air pollutants and greenhouse gases and "double-reach" (i.e., carbon peaks and air quality compliance) is on the agenda, which requires a better understanding of the characteristics of both greenhouse gas emissions and air pollutant emissions.

Several studies have investigated emissions of greenhouse gases in China, most of which focus on local areas. For instance, researches on carbon emission inventory are mainly in Beijing (Zhao et al., 2017), Shanghai (Shao et al., 2020), Nanjing (Bi et al., 2011), Guangzhou (Wu et al., 2021) and other megacities or urban groups (Liu et al., 2012; Sugar et al., 2012; Xu et al., 2018), making it difficult to analyze carbon emissions comprehensively in China. In contrast, very limited studies have conducted research on carbon emissions across China's cities partly due to data limitations. For example, Wang and Liu (2017) developed a city-level CO_2 emissions inventory in China for 1992–2013, however, the application of top-down methods may cause substantial biases in the estimation (Rayner et al., 2010; Cai et al., 2019). The bottom-up approach requires more detailed data of point source than a top-down approach while maximally ensuring the accuracy of emissions inventories. Wang and Cai (2017) compared three CO_2 emission inventories, including Emissions Database for Global Atmospheric Research (EDGAR; http://edgar.jrc.ec.europa.eu/), the Fossil Fuel Data Assimilation System (FFDAS; http://hpcg.purdue.edu/FFDAS/) and the China High Resolution Emission Gridded Data (CHRED; http://www.cityghg.com/), which are all based on bottom-up approaches. The comparisons showed that CHRED (10 km × 10 km) was in line most with the emission status of China. However, understanding carbon emissions alone is far from meeting the goal of co-benefits and double-reach, and building a list of air pollutant emissions is indispensable as well.

For emission inventories of air pollutants, more attentions have been paid to several regions and sectors where emissions are high, e.g. Beijing-Tianjin-Hebei region (Zheng et al., 2019), the Yangtze River Delta (YRD) region (Fu et al., 2013; Zhou et al., 2017; An et al., 2021), the Pearl River Delta (PRD) region (Zheng et al., 2009; Ou et al., 2015), or from the perspective of sectors, i.e., the power plant (Liu et al., 2015; Tang et al., 2019), the industry sector (Bo et al., 2017; Simayi et al., 2019). At the national level, the Multi-resolution Emission Inventory for China (MEIC; $0.25^{\circ} \times 0.25^{\circ}$; http://www.meicmodel.org) is developed by Tsinghua University to provide national emission inventory at five sectors with a spatial resolution of $0.25^{\circ} \times 0.25^{\circ}$. With the improvement of China's continuous emissions monitoring systems (CEMS) network such as the consideration of ultra-low emissions (ULE) standards policy, many studies point out that the use of CEMS data can get real-time and unit-specific emission factors (Tang et al., 2019; Zhang et al., 2019; Bo et al., 2020; Tang et al., 2020c).

Moreover, to the best of our knowledge, few studies have tried to use the same data sources to construct both greenhouse gas and air pollutant emissions, making it challenging to evaluate their concomitant control. In this study, combined with several databases such as CEMS, Environmental Statistics (ES), Emission Permit Implementation Report (EPIR) as well as National Bureau of Statistics (NBS), using the year of 2018 as an example, we construct a high resolution emission inventory of CO_2 and air pollutant in China. This multi-sector emission inventory, namely CHRED 3.0A, is an extension of our previous data set which is composed of greenhouse gas emissions only (CHRED 2.0; Cai et al., 2019). The newly developed CHRED 3.0A emission inventory includes nine air pollutants and carbon emissions from the same data source at a high resolution of 10-km, aiming to elucidate the spatial and temporal characteristics of CO_2 and air pollutant in China. The emission inventory will be made available at http://www.ieimodel.org/.

2. Method and data

The CHRED 3.0A emission inventory developed in this study is divided into five main sectors, including power, industry, transportation, resident and agriculture, with the sub-sectors and activity data shown in Table S1. The emissions of CO_2 and air pollutants in China are detailed below, and please note that due to data availability, emissions in Taiwan are not included.

2.1. CO_2 emissions

The method of deriving CO_2 emissions are based on an earlier version of CHRED (Wang et al., 2014; Cai et al., 2018a), which has been widely used in many studies (Cai et al., 2018b; Jing et al., 2018; Liu et al., 2019; Wu et al., 2021). CHRED, as well as the updated version CHRED 2.0, is based on a bottom-up approach that uses a massive amount of point source and survey data, with high accuracy and high-resolution carbon emissions dataset (Cai et al., 2019). Carbon emissions are divided into five main sectors (i.e., industry, transportation, agriculture, resident and service) in the database of CHRED, and have been adjusted to the corresponding emissions sectors used in this study (i.e., power, industry, transportation, agriculture

and resident). The detailed information on sector match can be seen in Table S2.

2.2. Air pollutant emissions

For emissions from air pollutants, two methods are used in this study, with one based on CEMS data (Method 1) and the other one based on the traditional method (Method 2). For Method I, emissions of air pollutants can be estimated according to Eqs. (1)–(3), whereas for Method II, they are estimated based on Eq. (4).

$$E_{i,j,m} = A_{i,m} EF_{i,j,m} \tag{1}$$

$$A_{i,m} = \frac{G_{p,m}}{\sum_{m=1}^{12} G_{p,m}} A_i \tag{2}$$

$$EF_{i,j,m,h} = C_{i,j,m,h} V_i \tag{3}$$

$$E_{s,j} = A_{s,j} \times EF_{s,j} \times \left(1 - \eta_{s,j}\right) \tag{4}$$

where i, j, p and s represent the unit of power plant or industry, pollutant type, province and emission sector, respectively; m and h stand for the month and hour, respectively; E is the emission of air pollutants (t), A and EF are the activity level and emission factor (kg per activity data), respectively. G indicates the power plant generation or the production of industrial processes, C and V represent the concentration of air pollutants (g/m^3) at the monitored stack and the theoretical flue gas rate (m^3 per activity data); η represent the emission sector and removal efficiency of air pollutants (%).

Only SO_2, NO_x, $PM_{2.5}$ and PM_{10} emissions from power plants and some industrial sectors (i.e., the production of iron and steel production, cement and lime) were estimated based on the Method I by using CEMS data. As the CEMS dataset provides direct, actual and real-time measurements of emission concentrations for SO_2, NO_x and PM at stacks in power plant and some industries across China, the unit-specific and hourly-frequent EF as well as the emissions could be obtained by this method (Tang et al., 2019; Tang et al., 2020a; Tang et al., 2020b). In addition, emissions from the remaining sectors were calculated using Method II.

2.2.1. Activity level

All activity level data are derived from ES, EPIR, CHRED, NBS (https://data.cnki.net/), CIIN (https://www.chyxx.com/), Landscan population dataset (https://landscan.ornl.gov/), etc. For example, activity data of the power sector and some sub-sectors of industry sector (i.e., the production of iron and steel, cement and glass) are derived from ES and the parameter of G in Eq. (2) can be derived from NBS directly. For the remaining industry sub-sectors, activity level data of industrial boilers and production of lime are derived from CHRED, while petrochemical related industries and other industrial sub-sectors (e.g., the production of coke, non-ferrous metals and other industrial processes) are obtained from EPIR and NBS, respectively. In terms of the sources of industrial solvent use, including printing and dyeing, surface coatings, pesticide use and other solvent use, they can be extracted from both NBS and CIIN. More specifically, the solvents used in printing and dyeing industry are divided into one kind of the dye and eight kinds of inks (i.e., flat ink, letterpress ink, flexographic ink, gravure ink, screen printing ink, UV ink, jet printing ink and other inks), the proportion of different inks refers to CIIN; The architectural coatings from the surface coating are also divided into two kinds (interior wall coatings and exterior wall coatings) according to the method described in Wei et al. (2008). It should be noted that since there is no statistics on the activity level data of some solvent use sub-sectors (e.g. printing and dyeing and architectural coatings), we use apparent consumption shown in Eq. (5) as activity data.

$$AC = P + In - Out \tag{5}$$

where *AC* represents the apparent consumption; *P*, *In* and *Out* indicate the production, input and output of the coating, respectively.

Activity data related to transportation sector are basically from CHRED with the exception of data in gasoline evaporation, which are derived from the motor vehicle population of NBS. In this sector, we divide it into on-road and non-road (i.e., waterway, aviation, railway, agricultural machinery and gasoline evaporation) emissions. The activity data of this sector, except for gasoline evaporative emissions, are the consumption of diesel, gasoline and natural gas of different vehicles or devices.

In terms of residential source emissions, there are three sub-sectors, namely biomass combustion, other residential burning and residential solvent use. The activity data on biomass burning are based on the crop yields (including paddy, wheat, sorghum and oil crop) and production-to-residue ratio of NBS. In contrast, activity data of other residential burning (including the consumption of residential coal and natural gas) are derived from CHRED directly and emissions from residential solvent use are calculated based on the urban population which is available at urban/rural extent data (Shen et al., 2017) and the Landscan database.

Finally, for the agricultural sector, the activity level data of nitrogen fertilizer application and livestock breeding are from NBS, while the activity data of human feces are the rural population which is available at the urban/rural extent data (Shen et al., 2017) and Landscan population data. For the use of nitrogen fertilizer, only the total consumption of nitrogen fertilizer is recorded in NBS, which is divided into urea, ammonium bicarbonate, ammonium nitrate, ammonium sulfate and other nitrogen fertilizers (Huang et al., 2012). In terms of the livestock breeding, we use the annual output as the activity level for pigs, chickens, ducks and geese, while the annual inventory of other livestock is adapted.

2.2.2. Emission factors

In order to reduce the uncertainty of emission factors, we select the emission factors that are in line with the local conditions of China as much as possible, such as Local measured data, Tsinghua University's Emission Inventory Manual (THUEIM) and a large number of literatures based on Chinese air pollutants emissions.

2.2.2.1. Power. The emission factors of some air pollutants (i.e., SO_2, NO_x, $PM_{2.5}$ and PM_{10}) are obtained by the concentration of air pollutants at the monitored stack and the theoretical flue gas rate (Eq. (3)). The concentration of these air pollutants is from CEMS data with hourly temporal resolution and the theoretical flue gas rate of different fuels can be derived from our previous studies (Qu et al., 2020; Tang et al., 2020b). For the remaining air pollutants (including VOCs, CO, BC, OC and NH_3), emission factors are derived from THUEIM according to different fuel types, boilers and installed capacity of a specific power plant.

2.2.2.2. Industry. For emissions from industrial boilers, the emission factors of CO, VOCs, NO_x and NH_3 are from the THUEMI, whereas factors of SO_2, $PM_{2.5}$, PM_{10}, BC and OC is obtained by Eqs. (5)–(8) based on the sulfur and ash content of fuel (Liu et al., 2015).

$$EF_{SO_2} = 2 \times S \times (1 - sr) \tag{5}$$

$$EF_{PM} = Aar \times (1 - ar) \times f_{PM} \tag{6}$$

$$EF_{BC} = EF_{PM_{2.5}} \times f_{BC} \tag{7}$$

$$EF_{OC} = EF_{PM_{2.5}} \times f_{OC} \tag{8}$$

where EF_{SO2}, EF_{PM}, EF_{BC} and EF_{OC} indicate the emission factor of SO_2, $PM_{2.5}$ or PM_{10}, BC and OC, respectively; *S* and Aar represent the sulfur and ash content in fuel (g/kg); *sr* and *ar* are the proportion of sulfur and ash into bottom ash (%); f_{PM} indicates the proportion of $PM_{2.5}$ or PM_{10} in total particulate matter, f_{BC} and f_{OC} are the proportion of BC and OC in $PM_{2.5}$.

In terms of industrial processes, the emission factors of SO_2, NO_x, $PM_{2.5}$ and PM_{10} for the sectors of cement production, iron and steel were

calculated by Eq. (3), while the emissions factors for all the other air pollutants are available at THUEIM. Only VOCs are emitted from solvent sources, with the emission factors from THUEIM and some published literatures, and the specific emission factors are listed in Table S3.

2.2.2.3. Transportation. The sector of transportation includes emissions from road and non-road. Road emissions mainly refer to the fuel (gasoline, diesel and gas) emissions of trucks, buses and other vehicles. The emission factors are from U.S. Environmental Protection Agency Compilation of Air Pollutant Emissions Factors, the joint European Monitoring and Evaluation Programme (EMEP) and European Environment Agency (EEA) datasets. In contrast, the emission factors of most non-road subsectors (i.e., rail, waterway and agricultural machinery) are from THUEIM, while that of gasoline evaporation is from EMEP.

2.2.2.4. Resident. Biomass combustion is an important portion of residential sources, accounting for the majority of PM and VOC emissions. In this study, the emission factors of residential solvent use and straw combustion, including open-air combustion and biomass fuel combustion, of paddy, wheat, sorghum and oil crop are derived from THUEIM. For the other residential combustion, including residential consumption of coal and natural gas, emission factors of coal and natural gas are derived from a large number of previous studies as well as THUEIM, with emission factors of household coal listed in Table S4.

2.2.2.5. Agriculture. The agricultural sector only emits ammonia, the emission factors of nitrogen fertilizer application vary according to different types of nitrogen fertilizer and soil pH, and that of livestock breeding depends on the type of livestock, the relevant emission factors refer to the study of Xu et al. (2015). By contrast, the emission of human feces is based on the number of rural population, and emission factors came from THUEIM.

2.2.3. Spatial distributions

In this study, we select point source data as much as possible, such as the point source information of power plants, iron and steel plants, cement plants, petrochemical related plants and so on, to reduce uncertainties of the emissions inventory. For the emission data without specific location information, we use the appropriate allocation index for spatial allocation. The specific allocation method is shown in Table S5. The Gross Domestic Product (GDP) and population data is provided by Data Center for Resources and Environmental Sciences, Chinese Academy of Sciences (RESDC) (http://www.resdc.cn).

3. Results

3.1. Emissions of CO_2 and air pollutants

The sectoral emissions of CO_2 and air pollutants including CO, NO_x, VOCs, SO_2, $PM_{2.5}$, PM_{10}, NH_3, BC and OC in China in 2018, derived in this study as well as from MEIC emissions (http://meicmodel.org/) are displayed in Fig. 1, with the sectoral emissions from this study shown in Table S6. The emissions between this study and MEIC indicate comparable magnitudes in general. It clearly shows that the major sectors for CO_2 emissions are power and industry, which are the primary contributors to majority of the air pollutant emissions as well, indicating the possibility to maximize the benefit by the mutual control of both CO_2 and air pollutant emissions. Fig. 1b shows the emission contributions of CO_2 and air pollutants across mainland China from the five major sources. Specifically, CO_2 emissions are closely related to the fuel consumption of the sector. The power sector, with the primary coal consumption, accounts for 46 % of carbon emissions, followed by the industry (35 %) and transportation (12 %). It is noteworthy that almost no CO_2 emissions are produced by sectors such as agriculture, which contributes substantially (i.e., more than 85 %) to NH_3, consistent with previous studies (Huang et al., 2012; Kang et al., 2016; Yu et al., 2020). In contrast, the main sectors of VOC emissions are industry and transportation, which are primary sectors for NO_x emissions

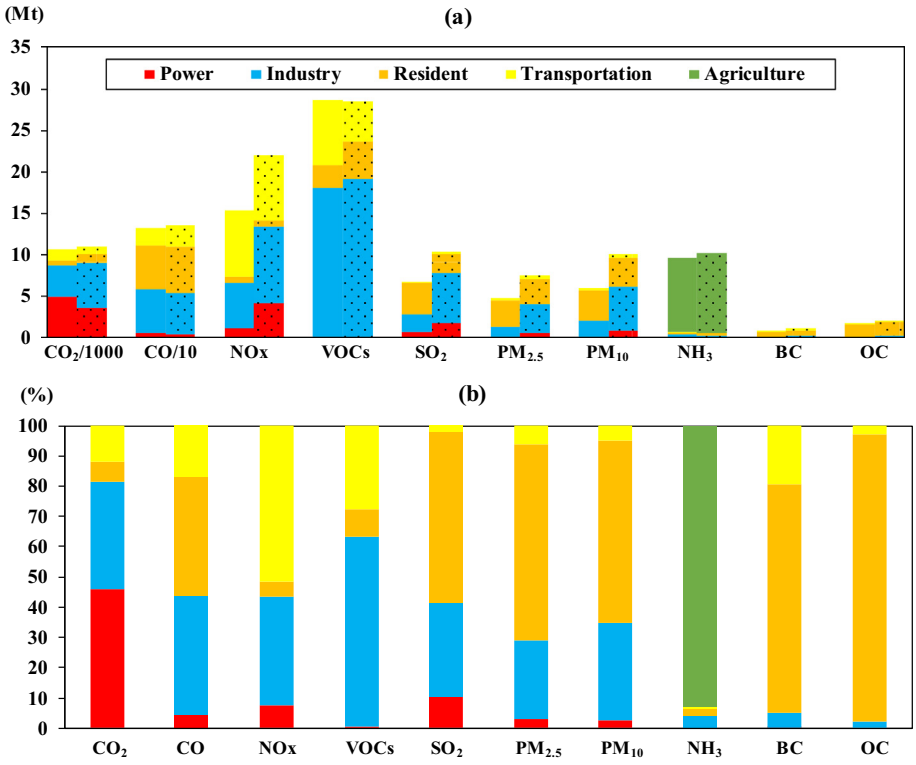


Fig. 1. (a) emission comparisons between this study (left bars) and that from MEIC (right bars with dots); (b) The fractional contributions of major sectors to CO_2 and air pollutants (including CO, NO_x, VOCs, SO_2, $PM_{2.5}$, PM_{10}, NH_3, BC and OC) emissions in 2018 in China.

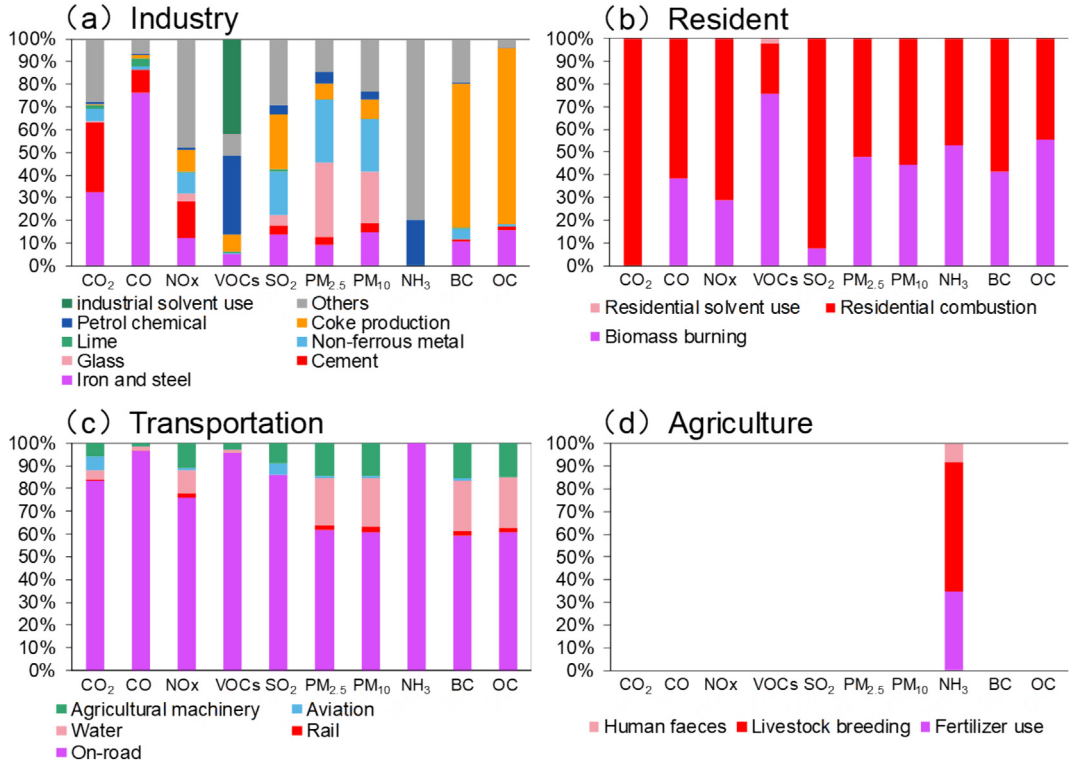


Fig. 2. The percentage contribution to CO_2 and air pollutant emissions at each sub-sector for industry, resident, transportation and agriculture.

as well, supported by a few previous studies (Sun et al., 2018; Zheng et al., 2018; An et al., 2021). Meanwhile, industry and resident are the major contributors to CO, SO_2, $PM_{2.5}$ and PM_{10}.

To more clearly view the sectoral emissions, the fractional contributions from all sub-sectors for industry, resident, transportation and agriculture are shown in Fig. 2. Industry is the major CO_2 emitter, with the largest emissions from sub-sectors of cement, iron and steel (Fig. 2a). These subsectors contribute a substantial portion to majority of air pollutants as well. For air pollutant species such as VOCs, the two major emitters are industry and transportation (Fig. 1), with the largest subsectors of solvent use and on-road transportation (Fig. 2a,c), comparable to the results shown previously (Zheng et al., 2018; An et al., 2021). In addition, the biomass burning and

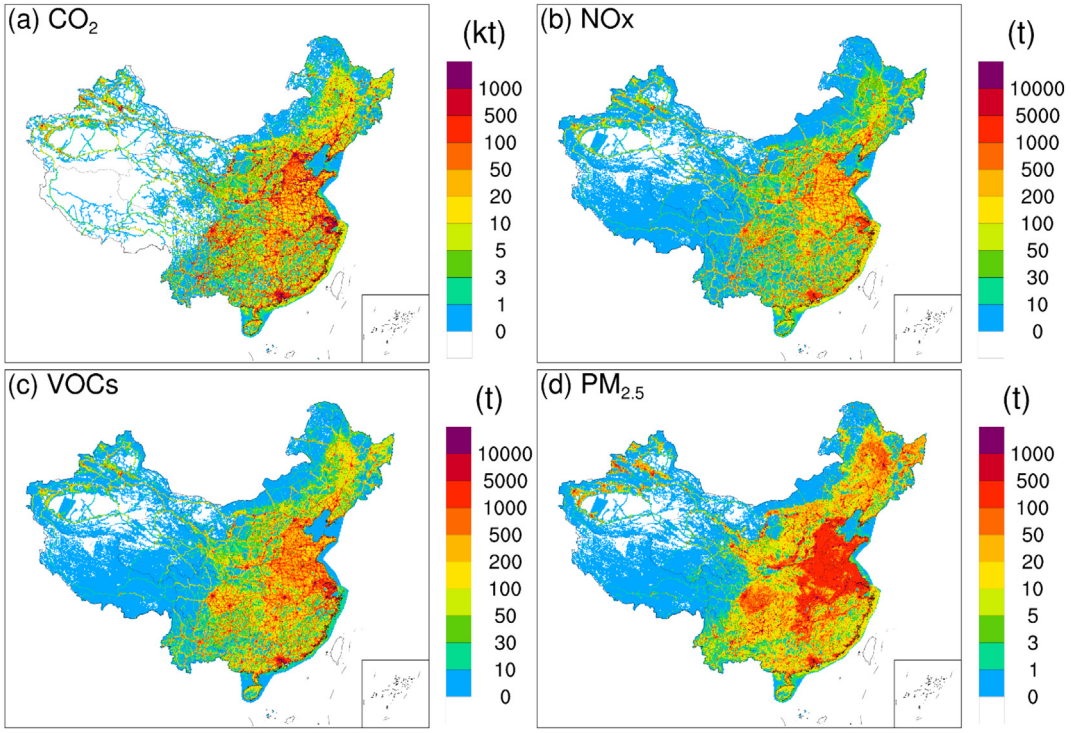


Fig. 3. Emissions of CO_2, NOx, VOCs and $PM_{2.5}$ at the horizontal resolution of 10 km*10 km in 2018.

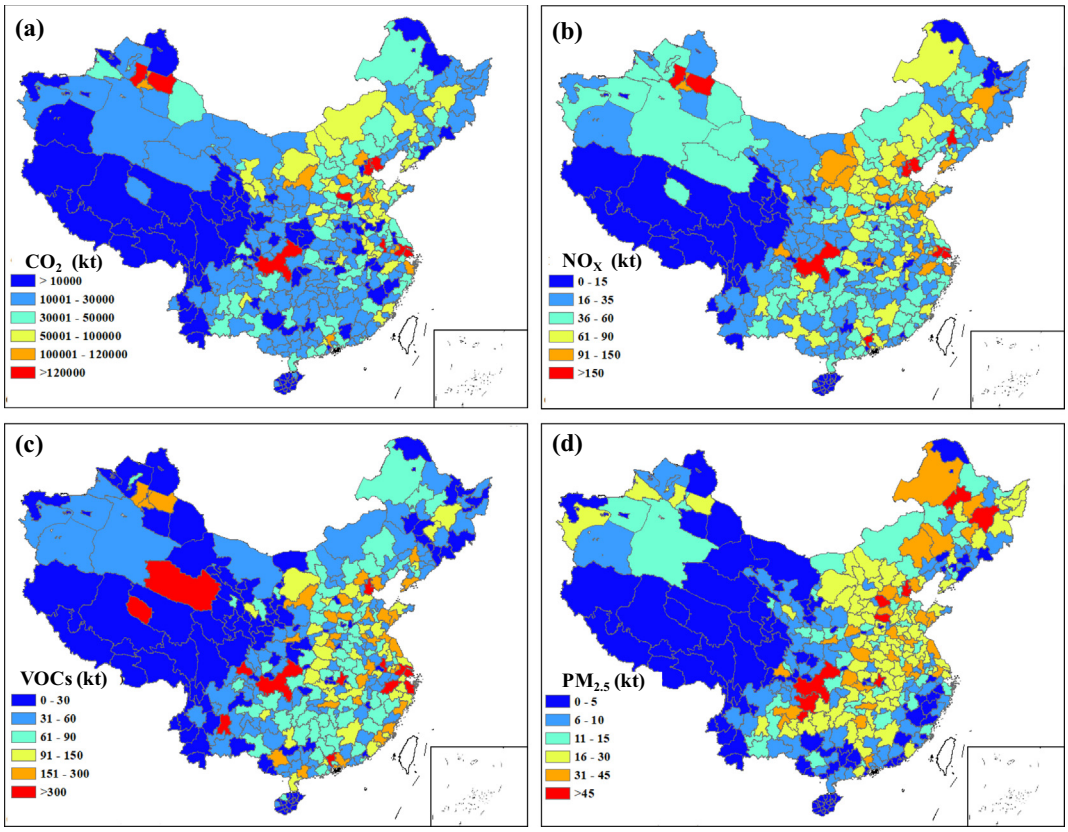


Fig. 4. Annual emissions at city-level for CO_2, NOx, VOCs and $PM_{2.5}$ in 2018.

residential combustion are the major residential sub-sectors (Fig. 2b), and the fertilizer use and livestock breeding are the major agriculture subsectors emitting NH_3.

The spatial distribution of emissions of CO_2, NOx, VOCs and $PM_{2.5}$ are shown in Fig. 3, with the other species, including CO, SO_2, PM_{10}, NH_3, BC and OC shown in Fig. S1. The spatial distributions of emissions vary dramatically, with emissions in eastern China much higher than that in the western China, and similar spatial distributions can be seen among all species. For instance, the emissions of all species in Northern China (Beijing, Tianjin, Hebei Province, Henan Province, Shandong Province, Inner Mongolia and Shanxi Province) and Eastern China (Shanghai, Jiangsu Province, Anhui Province, Zhejiang Province, Fujian Province, Jiangxi Province, Hubei Province and Hunan Province) exceed 50 % (53 %–64 %) of the national emissions, while they account for 30 % national area only. The CO_2 and air pollutant emissions at provincial level are shown in Table S7. Most of the species emissions are concentrated in industrial developed provinces, such as Shandong, Hebei, Jiangsu, Heilongjiang, etc., attributable to the fuel consumption of industry and power. Moreover, the striking

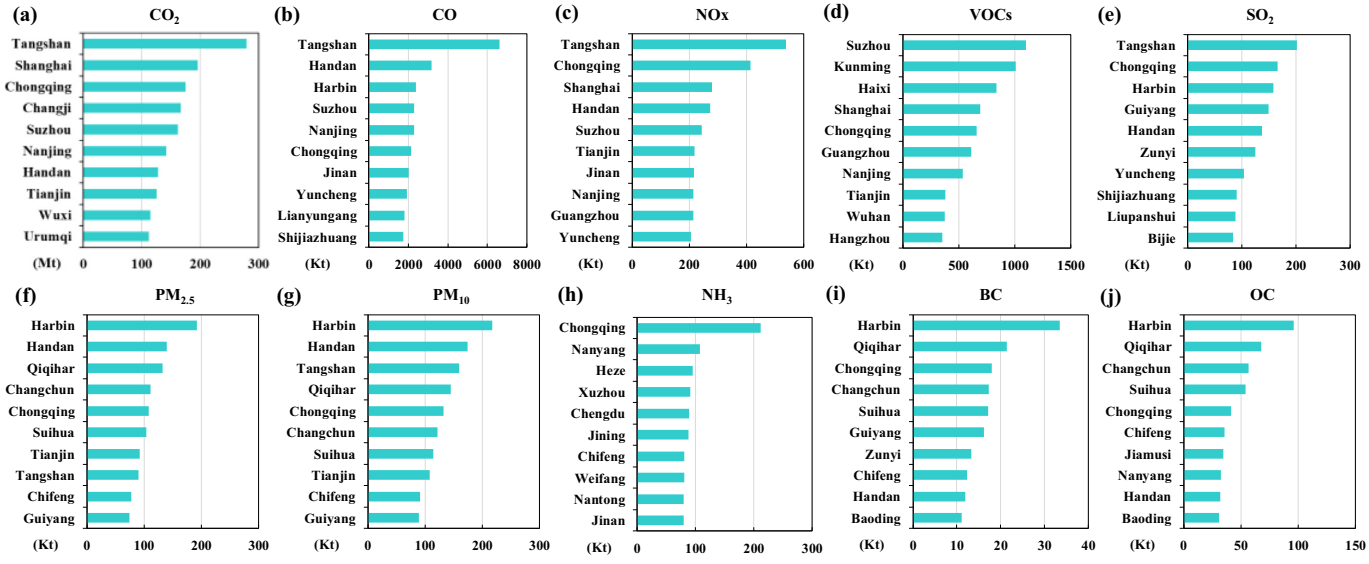


Fig. 5. Top 10 emitters for CO_2 and air pollutants.

feature is that the large spatial gradient is nicely delineated considering the bottom-up method applied in this study, which has been shown previously in Fig. 2A in Wang and Cai (2017), and the spatial distributions are more reasonable in representing the spatial heterogeneity compared to other dataset such as EDGAR and FFDAS (Fig. 2B,C in Wang and Cai, 2017).

3.2. Emission characteristics at the city-level, per GDP and capita

To further understand the emissions at the city-level, Fig. 4 shows annual emissions of CO_2, NOx, VOCs and $PM_{2.5}$ at prefectural cities in 2018, with emissions of the other six species (CO, SO_2, PM_{10}, NH_3, BC, OC) at Fig. S2. The top 10 cities for CO_2 and each air pollutant are listed in Fig. 5. The top ten CO_2 emitters were Shanghai, Tangshan, Beijing, Tianjin, Jining, Handan, Chongqing, Suzhou, Shijiazhuang and Wuhan in 2005 (Cai et al., 2019), whereas in 2018, the top 10 cities are Tangshan, Shanghai, Chongqing, Changji, Suzhou, Nanjing, Handan, Tianjin, Wuxi and Urumqi. It is noteworthy that the CO_2 emissions in Cai et al. (2019) include both the direct and indirect emissions, whereas the indirect emissions are those due to purchased electricity, and the emissions in this study only include those from direct emissions. For instance, for Beijing, the indirect CO_2 emissions account for 26 % (Cai et al., 2019), and without accounting for indirect CO_2 emissions in this study, Beijing ranked 11th in 2018, right below that in Urumqi.

The spatial distributions of emissions per GDP for CO_2, CO, NOx, VOCs, SO_2, $PM_{2.5}$, PM_{10}, NH_3, BC and OC are displayed in Fig. 6, with the probability distributions shown in Fig. 7. A comparable set of figures for emissions per capita is shown in Figs. S3 and S4. Overall, the spatial distribution of emissions per GDP indicates the strikingly spatial heterogeneity, with larger values over relatively less developed areas such as western China and northeastern China. Whereas over eastern China, the coastal areas where the economy are relatively well developed, exhibit the smallest emissions per GDP. Meanwhile, the probability distribution (Fig. 7) indicates the emissions per GDP span a few orders, emphasizing the existence of large spatial inhomogeneity. The spatial distribution and probability of emissions per capita for CO_2 and air pollutants, shown in Figs. S3 and S4, displaying comparable spatial characteristics in general.

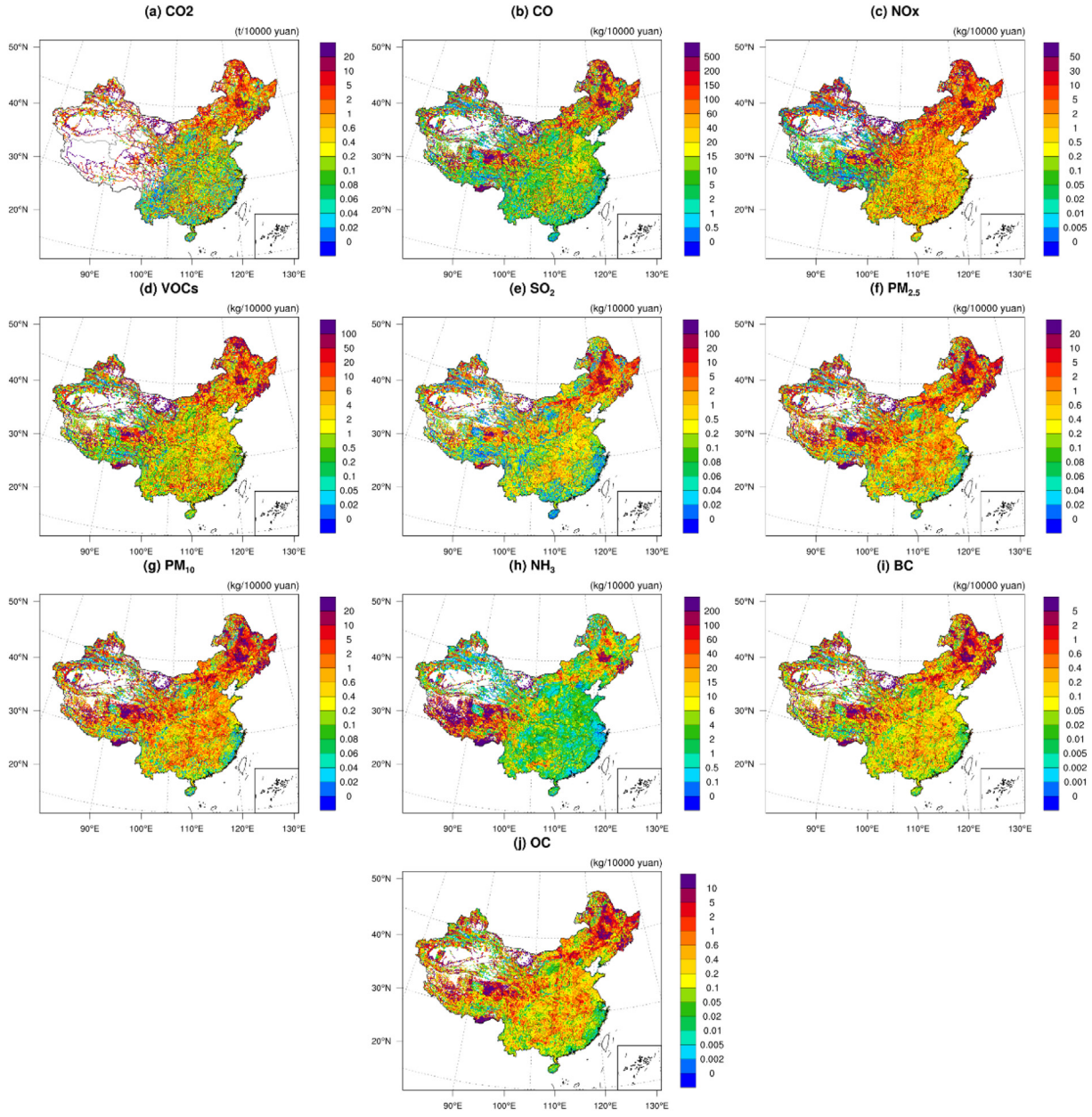


Fig. 6. Spatial distribution of emissions per GDP.

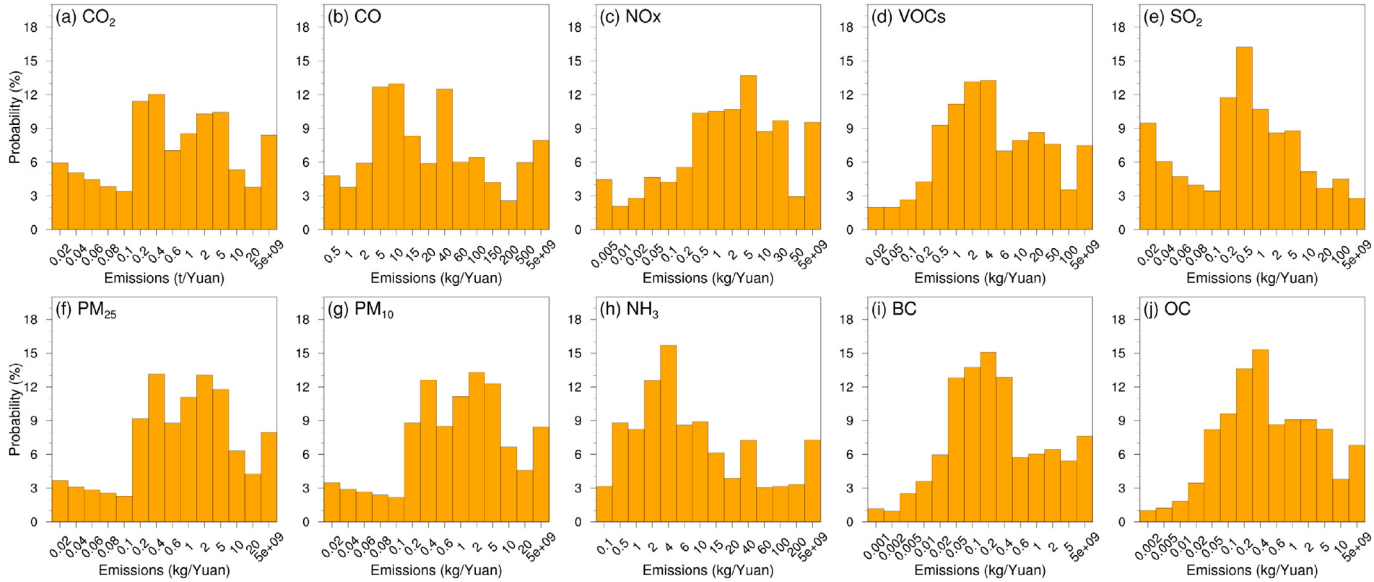


Fig. 7. Probability distributions of emissions per GDP (10,000 Yuan) in China for each species, including CO_2, CO, NO_x, VOCs, SO_2, $PM_{2.5}$, PM_{10}, NH_3, BC and OC. Please note that for each panel, the distribution is drawn based on all grids (10 km * 10km) over China.

3.3. Characterizing the spatial heterogeneity of CO_2 and air pollutant emissions

To further delve into the characterization of emission spatial heterogeneity, the probability distributions of CO_2 and air pollutants are shown in Fig. 8, with the cumulative distributions shown in Fig. S5. The distributions in general indicate that majority of the emissions are concentrated over a small area, while a large number of grids (purple line) only account for a small fraction (histograms). For instance, the number of grids account for 90 % of the total amount of emissions for CO_2, CO, NOx, VOCs, SO_2, $PM_{2.5}$, PM_{10}, NH_3, BC and OC are 5 %, 15 %, 16 %, 13 %, 10 %, 18 %, 17 %, 27 %, 22 % and 19 %, respectively. Meanwhile, the distributions of emissions from either CO_2 or air pollutants may behaves positively or negatively skewed.

To better understand the spatial consistency, the probability of emissions for each species based on the emission amount of CO_2 at the sectoral level is shown in Fig. 9. Please note that for each bin, the sample sizes and grids of all species are the same as CO_2. The grids exceeding 90 % of CO_2 emissions are those with grid level emissions larger than 0.17 Tg/year, and among all these grids, they contribute to 73 % for SO_2 emissions, followed by VOCs, CO, NOx, PM_{10}, $PM_{2.5}$, which all exceed 50 % and indicate strong spatial consistencies between the air pollutants and CO_2 emissions. For the rest of species like BC, OC, which are mainly from resident, and NH_3, mainly from agriculture, share smaller spatial consistencies. From the perspective of sectors, industry is a major sector contributing substantially for all those air pollutants displaying clear spatial consistency with CO_2 emissions, while power is a major sector as well, particularly for SO_2 and NO_x.

4. Conclusions

Through the construction of the high-resolution CO_2 and air pollutant emission inventory, namely CHRED 3.0A, we first identify the major sources of these emissions, including power and industry. Secondly, we illustrate the sub-sectoral distributions of emissions, i.e., the primary subsectors in industry for CO_2 emissions are cement, iron and steel. The analysis of

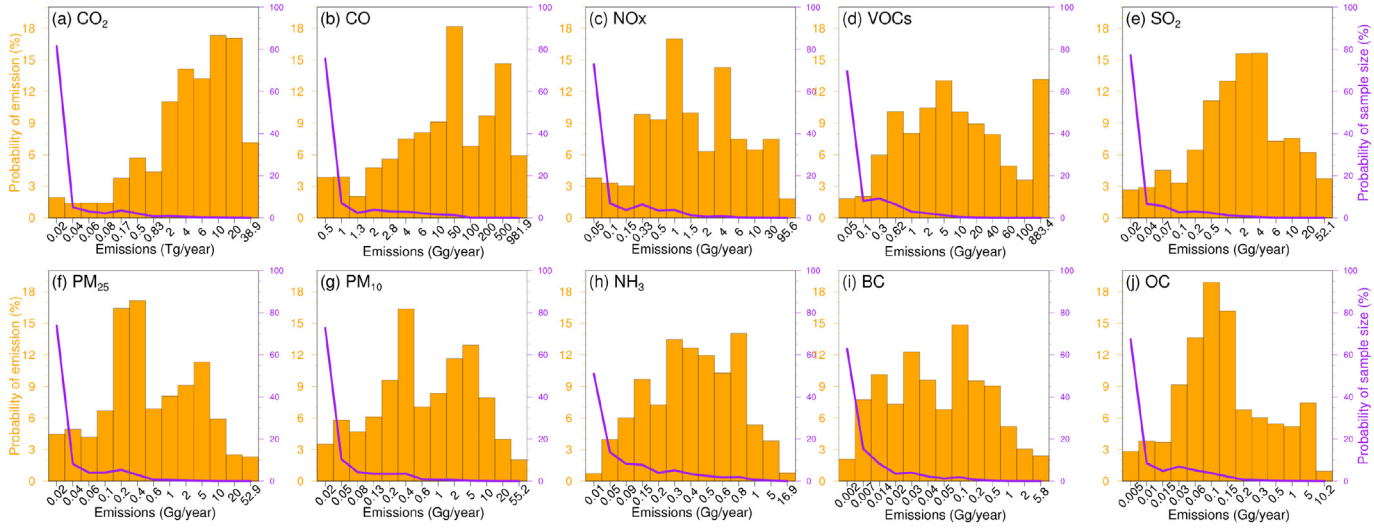


Fig. 8. The probability of emission amount in 2018 over all grids (at 10 km by 10 km) for each species, including CO_2, CO, NO_x, VOCs, SO_2, $PM_{2.5}$, PM_{10}, NH_3, BC and OC. Shown are the probability of emissions (left Y axis; Yellow bars) and the corresponding sample size (right Y axis; purple) for each bin of emission amount (X axis).

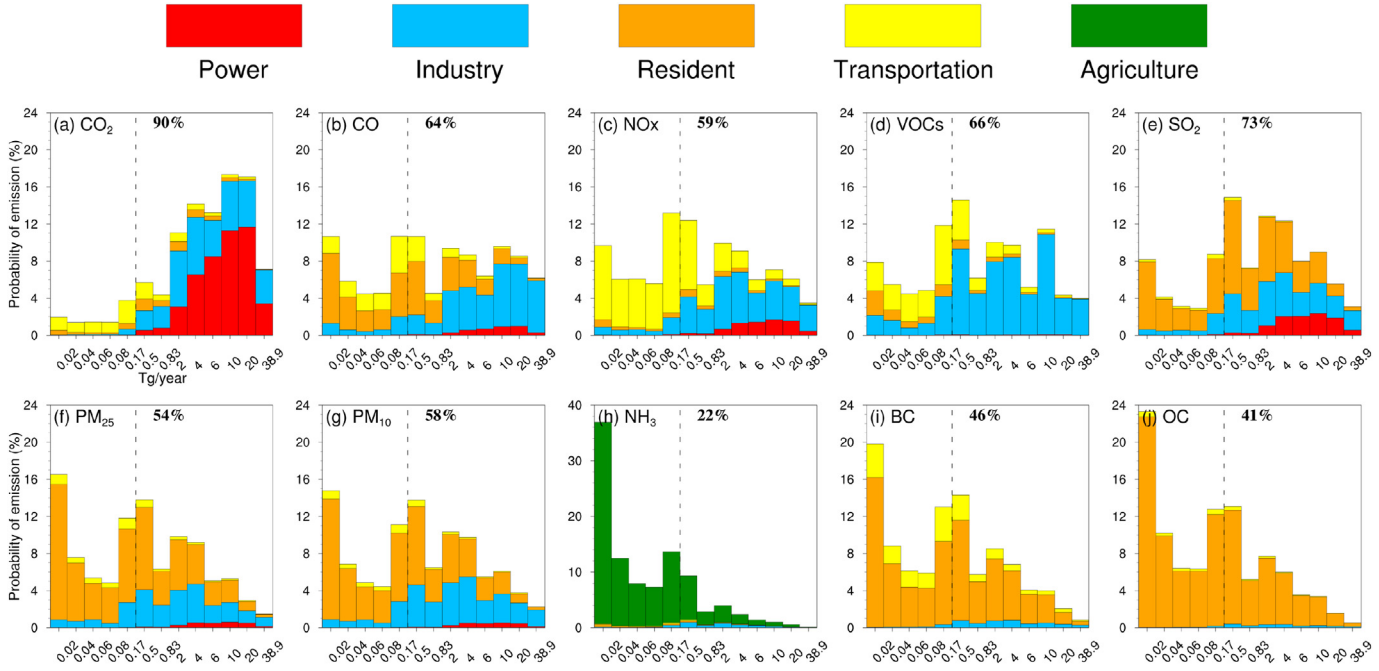


Fig. 9. The probability of sectoral emissions for each species, including CO_2, CO, NO_x, SO_2, VOCs, $PM_{2.5}$, PM_{10}, NH_3, BC and OC. Shown are the probability of emissions for each bin based on the emission amount of CO_2 (X axis). Note that for each bin, the sample sizes of all species are the same as CO_2. The dashed line indicates that 90 % of CO_2 is distributed on the right side of the line, with the numbers on the top right of each panel indicative of the corresponding emission fraction for different species in these grids.

the high-resolution spatial distribution indicates that for CO_2, 5 % of the grids account for 90 % of the total CO_2 emissions, indicative of the spatial heterogeneity. The spatial heterogeneity is clearly discernable for air pollutants as well, but with a lesser extent, ranging from 10 %–27 % of grids accounting for 90 % of the emissions. Moreover, the examination of spatial consistency reveals that for those grids accounting for 90 % of CO_2 emissions, they also contribute to more than 50 % of air pollutant emissions, which is substantially useful for the concomitant control of both these emissions, so as to achieve the carbon neutrality and improve air quality. In this study, we try our best to match the sectors for emissions of both greenhouse gases and air pollutants, which still has large room to improve in terms of the emission factors, sub-sectoral perspective, as well as species in particular of different VOC species, which inspires more studies in future. Nevertheless, the results presented in this study is substantially helpful for policy makers to make relevant strategies in regard of emission control of both greenhouse gas emissions and air pollutant emissions.

CRediT authorship contribution statement

Yang Gao: Formal analysis, Methodology, Writing – original draft. **Lei Zhang:** Formal analysis, Writing – original draft. **Aishi Huang:** Visualization. **Wenbin Kou:** Visualization. **Xin Bo:** Conceptualization, Methodology. **Bofeng Cai:** Conceptualization. **Jiabao Qu:** Visualization.

Data availability

The data that has been used is confidential.

Declaration of competing interest

The authors declare that they have no conflict of interest.

Acknowledgements

This research was supported by grants from the National Natural Science Foundation of China (42122039, 72174125) and Fundamental Research Funds for the Central Universities (buctrc202133).

Appendix A. Supplementary data

Supplementary data to this article can be found online at https://doi.org/10.1016/j.scitotenv.2022.157623.

References

An, J., Huang, Y., Huang, C., Wang, X., Yan, R., Wang, Q., Wang, H., Jing, S.a., Zhang, Y., Liu, Y., 2021. Emission inventory of air pollutants and chemical speciation for specific anthropogenic sources based on local measurements in the Yangtze River Delta region, China. Atmos. Chem. Phys. 21, 2003–2025. https://doi.org/10.5194/acp-21-2003-2021.

Bi, J., Zhang, R., Wang, H., Liu, M., Wu, Y., 2011. The benchmarks of carbon emissions and policy implications for China's cities: case of Nanjing. Energy Policy 39, 4785–4794. https://doi.org/10.1016/j.enpol.2011.06.045.

Bo, X., Zhen, R., Qu, J., Zhao, X., Tian, J., Zhang, H., Li, D., Zhou, B., 2017. Study on the management system of atmospheric pollutant emission inventory for steel industry of China. Environ. Pollut. Control 39, 578–582.

Bo, X., Li, Z.L., Qu, J.B., Cai, B.F., Zhou, B.H., Sun, L., Cui, W.G., Zhao, X.H., Tian, J., Kan, H., 2020. The spatial-temporal pattern of sintered flue gas emissions in iron and steel enterprises of China. J. Clean. Prod. 266. https://doi.org/10.1016/j.jclepro.2020.121667.

BP, 2020. BP Statistical Review of World Energy. http://www.bp.com/en/global/corporate/energy-economics/statistical-review-of-world-energy.html (last access: 8 June 2021).

Brock, C.A., Washenfelder, R.A., Trainer, M., Ryerson, T.B., Wilson, J.C., Reeves, J.M., Huey, L.G., Holloway, J.S., Parrish, D.D., Hubler, G., et al., 2002. Particle growth in the plumes of coal-fired power plants. J. Geophys. Res.Atmos. 107. https://doi.org/10.1029/2001jd001062.

Cai, B., Liang, S., Zhou, J., Wang, J., Cao, L., Qu, S., Xu, M., Yang, Z., 2018a. China high resolution emission database (CHRED) with point emission sources, gridded emission data, and supplementary socioeconomic data. Resour. Conserv. Recycl. 129, 232–239. https://doi.org/10.1016/j.resconrec.2017.10.036.

Cai, B., Wang, X., Huang, G., Wang, J., Cao, D., Baetz, B.W., Liu, L., Zhang, H., Fenech, A., Liu, Z., 2018b. Spatiotemporal changes of China's carbon emissions. Geophys. Res. Lett. 45, 8536–8546. https://doi.org/10.1029/2018gl079564.

Cai, B., Lu, J., Wang, J., Dong, H., Liu, X., Chen, Y., Chen, Z., Cong, J., Cui, Z., Dai, C., et al., 2019. A benchmark city-level carbon dioxide emission inventory for China in 2005. Appl. Energy 233, 659–673. https://doi.org/10.1016/j.apenergy.2018.10.016.

Chen, Q., Cai, B., Dhakal, S., Pei, S., Liu, C., Shi, X., Hu, F., 2017. CO2 emission data for chinese cities. Resources Conservation and Recycling 126, 198–208. https://doi.org/10.1016/j.resconrec.2017.07.011.

CSC, 2007. Eleventh Five Year Plan for National Environment Protection, China State Council (CSC), Beijing, China. http://www.gov.cn/zwgk/2007-11/26/content_815498.htm (last access: 8 June 2021).

CSC, 2013. Action Plan on Prevention and Control of Air Pollution, China State Council(CSC), Beijing, China. http://www.gov.cn/zwgk/2013-09/12/content_2486773.htm (last access: 8 June 2021).

Fu, X., Wang, S., Zhao, B., Xing, J., Cheng, Z., Liu, H., Hao, J., 2013. Emission inventory of primary pollutants and chemical speciation in 2010 for the Yangtze River Delta region, China. Atmos. Environ. 70, 39–50. https://doi.org/10.1016/j.atmosenv.2012.12.034.

Gao, Y., Zhang, L., Zhang, G., Yan, F., Zhang, S., Sheng, L., Li, J., Wang, M., Wu, S., Fu, J.S., et al., 2020. The climate impact on atmospheric stagnation and capability of stagnation indices in elucidating the haze events over North China plain and Northeast China. Chemosphere 258. https://doi.org/10.1016/j.chemosphere.2020.127335.

GBD 2019 Risk Factors Collaborators, 2020. Global burden of 87 risk factors in 204 countries and territories, 1990-2019: a systematic analysis for the Global Burden of Disease Study 2019. Lancet 396, 1223–1249. https://doi.org/10.1016/s0140-6736(20)30752-2.

Huang, X., Song, Y., Li, M., Li, J., Huo, Q., Cai, X., Zhu, T., Hu, M., Zhang, H., 2012. A high-resolution ammonia emission inventory in China. Glob. Biogeochem. Cycles 26. https://doi.org/10.1029/2011gb004161.

Jacob, D.J., Winner, D.A., 2009. Effect of climate change on air quality. Atmos. Environ. 43, 51–63.

Jimenez, J.L., Canagaratna, M.R., Donahue, N.M., Prevot, A.S.H., Zhang, Q., Kroll, J.H., DeCarlo, P.F., Allan, J.D., Coe, H., Ng, N.L., et al., 2009. Evolution of organic aerosols in the atmosphere. Science 326, 1525–1529. https://doi.org/10.1126/science.1180353.

Jing, Q., Bai, H., Luo, W., Cai, B., Xu, H., 2018. A top-bottom method for city-scale energy-related CO2 emissions estimation: a case study of 41 Chinese cities. J. Clean. Prod. 202, 444–455. https://doi.org/10.1016/j.jclepro.2018.08.179.

Kang, Y., Liu, M., Song, Y., Huang, X., Yao, H., Cai, X., Zhang, H., Kang, L., Liu, X., Yan, X., et al., 2016. High-resolution ammonia emissions inventories in China from 1980 to 2012. Atmos. Chem. Phys. 16, 2043–2058. https://doi.org/10.5194/acp-16-2043-2016.

Lau, L.C., Lee, K.T., Mohamed, A.R., 2012. Global warming mitigation and renewable energy policy development from the Kyoto protocol to the Copenhagen accord-a comment. Renew. Sust. Energ. Rev. 16, 5280–5284. https://doi.org/10.1016/j.rser.2012.04.006.

Li, M., Liu, H., Geng, G., Hong, C., Liu, F., Song, Y., Tong, D., Zheng, B., Cui, H., Man, H., et al., 2017. Anthropogenic emission inventories in China: a review. Natl. Sci. Rev. 4, 834–866. https://doi.org/10.1093/nsr/nwx150.

Liu, Z., Liang, S., Geng, Y., Xue, B., Xi, F.M., Pan, Y., Zhang, T.Z., Fujita, T., 2012. Features, trajectories and driving forces for energy-related GHG emissions from Chinese mega cites: the case of Beijing, Tianjin, Shanghai and Chongqing. Energy 37, 245–254. https://doi.org/10.1016/j.energy.2011.11.040.

Liu, F., Zhang, Q., Tong, D., Zheng, B., Li, M., Huo, H., He, K.B., 2015. High-resolution inventory of technologies, activities, and emissions of coal-fired power plants in China from 1990 to 2010. Atmos. Chem. Phys. 15, 13299–13317. https://doi.org/10.5194/acp-15-13299-2015.

Liu, F., Zhang, Q., Ronald, J.v.d.A., Zheng, B., Tong, D., Yan, L., Zheng, Y., He, K., 2016. Recent reduction in NOx emissions over China: synthesis of satellite observations and emission inventories. Environ. Research Letters 11. https://doi.org/10.1088/1748-9326/11/11/114002.

Liu, H., Nie, J., Cai, B., Cao, L., Wu, P., Pang, L., Wang, X., 2019. CO2 emissions patterns of 26 cities in the Yangtze River Delta in 2015: evidence and implications. Environ. Pollut. 252, 1678–1686. https://doi.org/10.1016/j.envpol.2019.06.102.

Ma, M., Gao, Y., Wang, Y., Zhang, S., Leung, L., Liu, C., Wang, S., Zhao, B., Chang, X., Su, H., et al., 2019. Substantial ozone enhancement over the North China plain from increased biogenic emissions due to heat waves and land cover in summer 2017. Atmospheric Chemistry and Physics Discussions 1–27. https://doi.org/10.5194/acp-2019-362.

Ou, J., Zheng, J., Li, R., Huang, X., Zhong, Z., Zhong, L., Lin, H., 2015. Speciated OVOC and VOC emission inventories and their implications for reactivity-based ozone control strategy in the Pearl River Delta region, China. Sci. Total Environ. 530, 393–402. https://doi.org/10.1016/j.scitotenv.2015.05.062.

Qu, J., Wang, P., Bo, X., Xue, X., Dong, G., Cui, L., Kang, M., Wang, T., Tang, L., Zhu, F., et al., 2020. Inventory and distribution characteristics of China's thermal power emissions under ultra-low reconstruction. Environ. Sci. 41, 93–99.

Rayner, P.J., Raupach, M.R., Paget, M., Peylin, P., Koffi, E., 2010. A new global gridded data set of CO2 emissions from fossil fuel combustion: methodology and evaluation. J. Geophys. Res.-Atmos. 115. https://doi.org/10.1029/2009jd013439.

Root, T.L., Price, J.T., Hall, K.R., Schneider, S.H., Rosenzweig, C., Pounds, J.A., 2003. Fingerprints of global warming on wild animals and plants. Nature 421, 57–60. https://doi.org/10.1038/nature01333.

Shao, L., Geng, Z., Wu, X.F., Xu, P., Pan, T., Yu, H., Wu, Z., 2020. Changes and driving forces of urban consumption-based carbon emissions: a case study of Shanghai. J. Clean. Prod. 245. https://doi.org/10.1016/j.jclepro.2019.118774.

Shen, H., Tao, S., Chen, Y., Ciais, P., Guneralp, B., Ru, M., Zhong, Q., Yun, X., Zhu, X., Huang, T., et al., 2017. Urbanization-induced population migration has reduced ambient PM2.5 concentrations in China. Science Advances 3. https://doi.org/10.1126/sciadv.1700300.

Sillman, S., 1999. The relation between ozone, NOx and hydrocarbons in urban and polluted rural environments. Atmos. Environ. 33, 1821–1845. https://doi.org/10.1016/s1352-2310(98)00345-8.

Simayi, M., Hao, Y., Li, J., Wu, R., Shi, Y., Xi, Z., Zhou, Y., Xie, S., 2019. Establishment of county-level emission inventory for industrial NMVOCs in China and spatial-temporal characteristics for 2010–2016. Atmos. Environ. 211, 194–203. https://doi.org/10.1016/j.atmosenv.2019.04.064.

Stanaway, J.D., Afshin, A., Gakidou, E., Lim, S.S., Abate, D., Abate, K.H., Abbafati, C., Abbasi, N., Abbastabar, H., Abd-Allah, F., et al., 2018. Global, regional, and national comparative risk assessment of 84 behavioural, environmental and occupational, and metabolic risks or clusters of risks for 195 countries and territories, 1990–2017: a systematic analysis for the global burden of disease study 2017. Lancet 392, 1923–1994. https://doi.org/10.1016/s0140-6736(18)32225-6.

Sugar, L., Kennedy, C., Leman, E., 2012. Greenhouse gas emissions from chinese cities. J. Ind. Ecol. 16, 552–563. https://doi.org/10.1111/j.1530-9290.2012.00481.x.

Sun, W., Shao, M., Granier, C., Liu, Y., Ye, C.S., Zheng, J.Y., 2018. Long-term trends of anthropogenic SO2, NOx, CO, and NMVOCs emissions in China, earth. Future 6, 1112–1133. https://doi.org/10.1029/2018ef000822.

Tang, L., Qu, J., Mi, Z., Bo, X., Chang, X., Anadon, L.D., Wang, S., Xue, X., Li, S., Wang, X., et al., 2019. Substantial emission reductions from chinese power plants after the introduction of ultra-low emissions standards. Nat. Energy 4, 929–938. https://doi.org/10.1038/s41560-019-0468-1.

Tang, L., Xue, X., Jia, M., Jing, H., Wang, T., Zhen, R., Huang, M., Tian, J., Guo, J., Li, L., et al., 2020a. Iron and steel industry emissions and contribution to the air quality in China. Atmos. Environ. 237. https://doi.org/10.1016/j.atmosenv.2020.117668.

Tang, L., Xue, X., Qu, J., Mi, Z., Bo, X., Chang, X., Wang, S., Li, S., Cui, W., Dong, G., 2020b. Air pollution emissions from chinese power plants based on the continuous emission monitoring systems network. Sci. Data 7. https://doi.org/10.1038/s41597-020-00665-1.

Tang, L., Xue, X.D., Jia, M., Jing, H., Wang, T., Zhen, R.Q., Huang, M.T., Tian, J., Guo, J., Li, L., et al., 2020c. Iron and steel industry emissions and contribution to the air quality in China. Atmos. Environ. 237. https://doi.org/10.1016/j.atmosenv.2020.117668.

Tylianakis, J.M., Didham, R.K., Bascompte, J., Wardle, D.A., 2008. Global change and species interactions in terrestrial ecosystems. Ecol. Lett. 11, 1351–1363. https://doi.org/10.1111/j.1461-0248.2008.01250.x.

Wang, M., Cai, B., 2017. A two-level comparison of CO2 emission data in China: evidence from three gridded data sources. J. Clean. Prod. 148, 194–201. https://doi.org/10.1016/j.jclepro.2017.02.003.

Wang, S., Liu, X., 2017. China's city-level energy-related CO2 emissions: spatiotemporal patterns and driving forces. Appl. Energy 200, 204–214. https://doi.org/10.1016/j.apenergy.2017.05.085.

Wang, J., Cai, B., Zhang, L., Cao, D., Liu, L., Zhou, Y., Zhang, Z., Xue, W., 2014. High resolution carbon dioxide emission gridded data for China derived from point sources. Environ. Sci. Technol. 48, 7085–7093. https://doi.org/10.1021/es405369r.

Wang, J., Zhao, B., Wang, S., Yang, F., Xing, J., Morawska, L., Ding, A., Kulmala, M., Kerminen, V.-M., Kujansuu, J., et al., 2017. Particulate matter pollution over China and the effects of control policies. Sci. Total Environ. 584, 426–447. https://doi.org/10.1016/j.scitotenv.2017.01.027.

Wei, W., Wang, S., Chatani, S., Klimont, Z., Cofala, J., Hao, J., 2008. Emission and speciation of non-methane volatile organic compounds from anthropogenic sources in China. Atmos. Environ. 42, 4976–4988. https://doi.org/10.1016/j.atmosenv.2008.02.044.

Wu, P., Guo, F., Cai, B., Wang, C., Lv, C., Liu, H., Huang, J., Huang, Y., Cao, L., Pang, L., et al., 2021. Co-benefits of peaking carbon dioxide emissions on air quality and health, a case of Guangzhou, China. J. Environ. Manag. 282. https://doi.org/10.1016/j.jenvman.2020.111796.

Xie, Y., Dai, H., Zhang, Y., Wu, Y., Hanaoka, T., Masui, T., 2019. Comparison of health and economic impacts of PM2.5 and ozone pollution in China. Environ. Int. 130. https://doi.org/10.1016/j.envint.2019.05.075.

Xing, J., Wang, S.X., Jang, C., Zhu, Y., Hao, J.M., 2011. Nonlinear response of ozone to precursor emission changes in China: a modeling study using response surface methodology. Atmos. Chem. Phys. 11, 5027–5044. https://doi.org/10.5194/acp-11-5027-2011.

Xu, P., Zhang, Y., Gong, W., Hou, X., Kroeze, C., Gao, W., Luan, S., 2015. An inventory of the emission of ammonia from agricultural fertilizer application in China for 2010 and its high-resolution spatial distribution. Atmos. Environ. 115, 141–148. https://doi.org/10.1016/j.atmosenv.2015.05.020.

Xu, X., Huo, H., Liu, J., Shan, Y., Li, Y., Zheng, H., Guan, D., Ouyang, Z., 2018. Patterns of CO2 emissions in 18 central chinese cities from 2000 to 2014. J. Clean. Prod. 172, 529–540. https://doi.org/10.1016/j.jclepro.2017.10.136.

Yu, X., Shen, L., Hou, X., Yuan, L., Pan, Y., An, J., Yan, S., 2020. High-resolution anthropogenic ammonia emission inventory for the Yangtze River Delta, China. Chemosphere 251. https://doi.org/10.1016/j.chemosphere.2020.126342.

Zeng, Y., Cao, Y., Qiao, X., Seyler, B.C., Tang, Y., 2019. Air pollution reduction in China: recent success but great challenge for the future. Sci. Total Environ. 663, 329–337. https://doi.org/10.1016/j.scitotenv.2019.01.262.

Zhang, Y., Bo, X., Zhao, Y., Nielsen, C.P., 2019. Benefits of current and future policies on emissions of China's coal-fired power sector indicated by continuous emission monitoring. Environ. Pollut. 251, 415–424. https://doi.org/10.1016/j.envpol.2019.05.021.

Zhao, L., Zhao, T., Wang, Y., 2017. A multisectoral decomposition analysis of Beijing carbon emissions. Clean Techn. Environ. Policy 19, 565–575. https://doi.org/10.1007/s10098-016-1249-1.

Zheng, J., Zhang, L., Che, W., Zheng, Z., Yin, S., 2009. A highly resolved temporal and spatial air pollutant emission inventory for the Pearl River Delta region, China and its uncertainty assessment. Atmos. Environ. 43, 5112–5122. https://doi.org/10.1016/j.atmosenv.2009.04.060.

Zheng, B., Tong, D., Li, M., Liu, F., Hong, C., Geng, G., Li, H., Li, X., Peng, L., Qi, J., et al., 2018. Trends in China's anthropogenic emissions since 2010 as the consequence of clean air actions. Atmos. Chem. Phys. 18, 14095–14111. https://doi.org/10.5194/acp-18-14095-2018.

Zheng, H.T., Cai, S.Y., Wang, S.X., Zhao, B., Chang, X., Hao, J.M., 2019. Development of a unit-based industrial emission inventory in the Beijing-Tianjin-Hebei region and resulting improvement in air quality modeling. Atmos. Chem. Phys. 19, 3447–3462.

Zhou, Y.D., Zhao, Y., Mao, P., Zhang, Q., Zhang, J., Qiu, L.P., Yang, Y., 2017. Development of a high-resolution emission inventory and its evaluation and application through air quality modeling for Jiangsu Province, China. Atmos. Chem. Phys. 17, 211–233.